Early Events of Pepsinogen Activation†

Henry E. Auer* and David M. Glick*

ABSTRACT: Stopped-flow measurements both with native pig pepsinogen and with a fluorescent derivative, labeled near the carboxyl terminus with a toluidinylnaphthalenesulfonyl (TNS) group at Lys_{364}, show rapid fluorescence changes following acidification. The rate constants observed by intrinsic fluorescence of the native zymogen are distinctly greater than those exhibited by the TNS derivative in the pH range examined. The rate constants for two early events in the activation of the derivative increase as the pH decreases from pH 3 to pH 2. The fluorescent intensities of these two processes also vary with pH. Because the ratios of these amplitudes fit the Henderson–Hasselbalch equation, it is concluded that the two processes represent concurrent events, rather than sequential ones. It is proposed that a protonation separates two forms of the zymogen. The conjugate acid undergoes the slower event, whereas the conjugate base, which predominates at pH 3, undergoes the faster event. It is proposed that both these pathways result in activation.

Pig pepsinogen activation at pH 3 and below is initiated by an acid-induced, unimolecular cleavage of the Leu_{16}–Ile_{17} peptide bond. The resulting protein, shortened by 16 residues, is pseudopepsin. It can continue the activation process by acting upon its neighboring molecules and removing an additional peptide, 17–44, producing pepsin (Al-Janabi et al., 1972). The rate of activation has conventionally been taken to be the rate at which potential activity of an acidified solution becomes pH 8.5 labile, because both pepsin and pseudopepsin, unlike pepsinogen, are irreversibly denatured at this pH. It is unknown, however, whether this phenomenom reflects the rate of bond cleavage or of a conformational change that precedes it. The rate of dissociation of the activation peptide has been shown to be slower by an order of magnitude than the rate of activation for a spin-labeled pepsinogen (Twining et al., 1981). Dissociation, therefore, may safely be put aside when the events that precede or are inseparably associated with the rate-limiting step are considered. There have been some reports of early conformational changes following acidification, but these were, admittedly, beyond the capabilities of the experimental methods that were applied to them at the time (Wang & Edelman, 1971; McPhie, 1972). Therefore, it is pertinent to inquire further into the early events of pepsinogen activation.

We expected that acidification would produce significant conformational changes in pepsinogen, even before the rate-limiting step of activation. In order to investigate this possibility, we have carried out fluorescence-detected stopped-flow kinetic studies on the early events following the exposure of pepsinogen to acid, using both the intrinsic fluorescence of the aromatic amino acid residues and that of an extrinsic probe. Wang & Edelman (1971) had shown that TNS-OH[1] fluoresces more strongly in the presence of pepsin than it does in the presence of pepsinogen, and this appeared to us to be a sensitive and convenient parameter for following activation. We were concerned, however, about the possibility that fluorescence changes due to association of TNS-OH and protein might be difficult to distinguish from changes in the protein after TNS-OH binding. Therefore, we sought to attach the fluorescent group covalently to the protein using a sulfonyl chloride derivative, which would react with nucleophilic groups of proteins, particularly with the amino groups. We have thus prepared TNS–pepsinogen, with the label covalently attached to the single ϵ-amino group that persists after removal of the activation peptide and have proceeded to study the kinetics of its activation by stopped-flow techniques.

Experimental Procedures

Materials. Pig pepsinogen was purchased from Sigma Chemical Co.; pepstatin was from Bristol Laboratories. 6-(*p*-Toluidinyl)naphthalene-2-sulfonyl chloride was purchased from Molecular Probes.

General Methods. Pepsin activity was assayed according to Chow & Kassell (1968), and activation of pepsinogen was followed by the method of Al-Janabi et al. (1972). Amino acid analysis was performed on a Dionex instrument.

Preparation of TNS–Pepsinogen. The fluorescent label was attached to pepsinogen by reacting 31.8 mg of the protein (0.8 μmol) in 46 mL of 0.1 M phosphate buffer, pH 7.5, 0 °C, with 1.06 mg of TNS-Cl (3.2 μmol) in 0.37 mL of DMF. After a 15-min reaction time the solution was dialyzed against water for 60 min and then extensively against several changes of 1 mM ammonium bicarbonate. Finally, the preparation was lyophilized.

Stopped-Flow Kinetic Measurements. Fluorescence-detected stopped-flow measurements were made by using an Aminco-Morrow stopped-flow module equipped with the Aminco fluorescence detection accessory, which captures light emitted at right angles to the incident light beam. Fluorescence was excited with a 75-W xenon arc light source. Wavelengths were chosen with a Bausch & Lomb 33-86-25 grating monochromator fitted with 9.6-nm band-pass slits. Intrinsic fluorescence was excited at 280 nm and isolated by a Corning 7-59 filter, which passes light above 305 nm. TNS fluorescence was excited at 366 nm. The emission was passed through a Wratten 2A filter, which transmits light above 415 nm. The stopped-flow mixing time was determined to be 3 ms. The temperature of the stopped-flow apparatus was regulated by a circulating water bath and monitored with a Tekmar RA-100 thermocouple thermometer. Reactions were initiated by 1:1 mixing of solutions of protein in 0.05 M glycine–0.2 M NaCl with HCl solutions in 0.2 M NaCl, whose

† From the Department of Biochemistry, Medical College of Wisconsin, Milwaukee, Wisconsin 53226. *Received October 12, 1983.* A preliminary report of this work was presented at the 74th Annual Meeting of the American Society of Biological Chemists, San Francisco, CA, June 1983 (Auer & Glick, 1983).

[1] Abbreviations: DMF, dimethylformamide; TNS, 6-(*p*-toluidinyl)-naphthalene-2-sulfonyl; TNS-OH, toluidinylnaphthalenesulfonate or -sulfonic acid; TNS-Cl, toluidinylnaphthalenesulfonyl chloride; TNS-NH_2, toluidinylnaphthalenesulfonamide.

0006-2960/84/0423-2735$01.50/0

acid concentrations were adjusted to yield desired pH values. Actual pH values were determined after the stopped-flow experiments on pooled samples of the product solutions. The kinetic transients were recorded with a Nicolet Explorer III digital oscilloscope interfaced to a Hewlett-Packard 9825 desktop computer. The results were smoothed by using the procedure of Savitzky & Golay (1964) and then transmitted to a Perkin-Elmer 3230 computer. The data were analyzed by subjecting them to nonlinear regression analysis for a one- or two-term exponential decay process.

Results

In order to estimate the number of TNS groups in the modified protein from its ultraviolet spectrum, we prepared TNS-NH_2 by dissolving 0.5 mg of TNS-Cl in 0.2 mL of DMF and then adding 2.0 mL of concentrated NH_3. This was shaken 20 min at room temperature, partially neutralized with concentrated HCl, and extracted into methylene chloride. This phase was washed with water, dried over anhydrous Na_2SO_4, and evaporated to dryness. The resulting TNS-NH_2 was taken up in a small volume of DMF and diluted to 0.1% DMF with 50% ethanol, a solvent that was felt would appropriately mimic the environment of the TNS groups on the protein. The ultraviolet absorption of TNS-NH_2 in this solvent was recorded. A correction for the TNS absorption of the modified protein at 280 nm was calculated and applied to the TNS–pepsinogen spectrum to obtain the net absorption due to the protein. Using the extinction coefficients reported for TNS-OH by McClure & Edelman (1966) and for pepsinogen by Perlmann (1964), we calculate that TNS–pepsinogen has 0.89 TNS group per molecule. TNS–pepsinogen prepared by longer reaction times with the same concentration of TNS-Cl produced a derivative with the identical spectrum.

In order to locate the site of substitution of the TNS group, the derivative was activated (2 mg in 1 mL of 0.05 M glycine hydrochloride and 0.2 M NaCl, 23 °C for 75 min) in the presence and in the absence of the pepsin inhibitor, pepstatin (0.1 mM). The activation mixtures were made alkaline with ammonium bicarbonate and then passed over a 0.8 × 17.5 cm Sephadex G-25 (Pharmacia) column, eluted with water. It was monitored for absorbance at 280 nm and for TNS fluorescence after dilution with an equal volume of DMF. The eluate was separated into a protein and a peptide fraction. In the absence of pepstatin about 80% of the TNS fluorescence eluted with the protein, but some appeared where activation peptides would be expected. In the presence of pepstatin, however, all the fluorescence cochromatographed with protein. We interpret these results to mean that the activation peptides contained no fluorescent label and that the small amount that appeared from the non-pepstatin-containing sample was due to autodigestion of TNS–pepsin.

The TNS–pepsin obtained from the activation in the absence of pepstatin was hydrolyzed for 24 h at 110 °C in 6 M HCl and subjected to amino acid analysis. The sample contained less than 0.1 lysine per pepsin molecule. (Pepsin contains only one lysine residue.)

TNS–pepsinogen was found to be activatable. Its rate of activation is of the same order of magnitude as that of native pepsinogen, and its pH dependence also resembles that of the native zymogen (Figure 1). The resulting proteolytic activity was the same as that derived from an equal weight of native pepsinogen.

Stopped-flow kinetic studies monitored by intrinsic fluorescence of the aromatic residues were carried out in the pH range between 2.16 and 2.97. At all pH values examined, a rapid decrease in fluorescent intensity, corresponding to

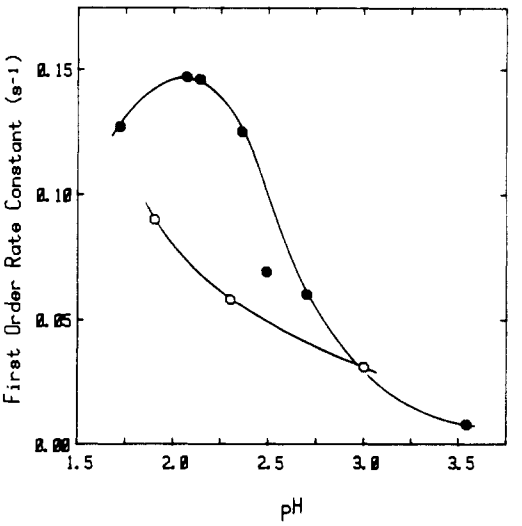

FIGURE 1: Rate of activation of zymogens vs. pH. Rates of activation at 22 °C were determined on 0.5 mg of zymogen by the method of Al-Janabi et al. (1972). First-order rate constants were extracted from semilog plots of these data. (●) TNS–pepsinogen. (○) Native pepsinogen.

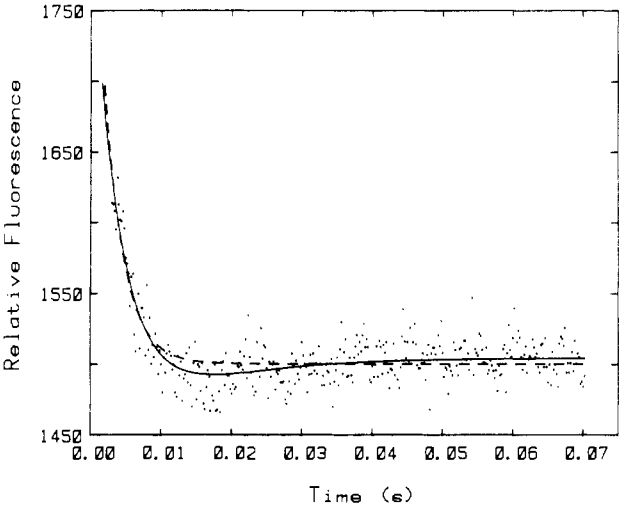

FIGURE 2: Example of a stopped-flow experiment obtained by observing the intrinsic fluorescence of native pepsinogen. A solution of pepsinogen, A_{280} = 0.42, in 0.05 M glycine–0.2 M NaCl, was mixed with an equal volume of dilute HCl in 0.2 M NaCl, to produce a pH of 2.36. The raw data shown were smoothed and then analyzed as described under Experimental Procedures. (---) The data were fitted to a one-term exponential described by Y_∞ = 1500, A = 407, and k = 359 ± 19 s^{-1}; the mean square residual = 44.2. (—) The data were fitted to a two-term exponential described by Y_∞ = 1505, A_f = 392, k_f = 235 ± 6 s^{-1}, A_s = −83, and k_s = 86 ± 4 s^{-1}; the mean square residual = 19.4. The symbol Y_∞ is the fluorescence intensity at infinite time, A is the amplitude, k is the first-order rate constant, and the subscripts f and s refer to the fast and slow events, respectively. On the fluorescence scale shown, the dark current was −1855.

12–15% of the initial value, was observed. In addition the three lowest pH values exhibited a second, slower phase of considerably weaker amplitude in the direction of an increase in intensity. An example of such a transient is shown in Figure 2. This curve was subjected to analysis according to both a one-term and a two-term exponential equation. As may be seen from the results given in the figure legend, the two-term analysis gives a significantly better fit to the data. The rate constants obtained in these experiments, analyzed according to a one-term or a two-term exponential decay, as appropriate, are presented on a logarithmic scale in Figure 3. The rate constants for the rapid phase are strongly dependent on pH, increasing in a monotonic fashion by a factor of almost 10 as

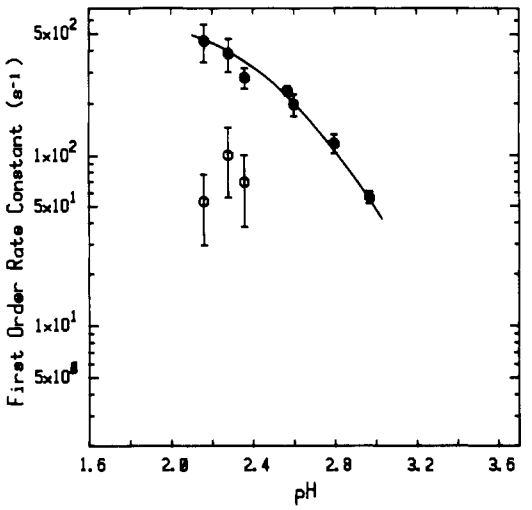

FIGURE 3: Rate constants for change in fluorescence of native pepsinogen vs. pH. First-order rate constants (±SD) for the fast event (●) and, when present, for the slow event (○), determined as in Figure 2, are shown as a function of pH.

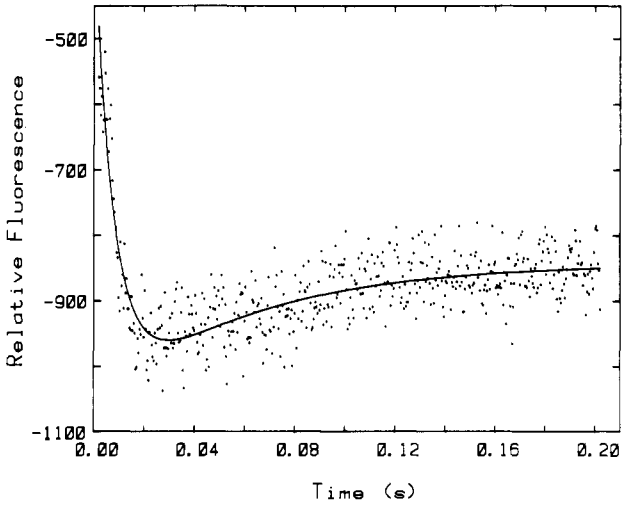

FIGURE 4: Example of a stopped-flow experiment using TNS–pepsinogen. A solution of TNS–pepsinogen, A_{366} = 0.083, in 0.05 M glycine–0.2 M NaCl, was mixed with an equal volume of dilute HCl in 0.2 M NaCl, to produce a solution of pH 2.48. The raw data shown here were smoothed and analyzed as described under Experimental Procedures. The fitted curve is described by $Y_\infty = -843$, $A_f = 743.3$, $k_f = 125.0 \pm 5.6$ s^{-1}, $A_s = -224.5$, and $k_s = 17.0 \pm 1.6$ s^{-1}, where the symbols have the same meaning as in Figure 2. On the fluorescence scale shown, the dark current was +1900.

the pH decreases from 2.97 to 2.16. Because of poor signal to noise characteristics, the rate constants for the slow phase have large standard deviations; over the narrow pH range in which they occur no trend with pH is apparent. In addition, the experiments at pH 2.57 and 2.60 gave hints of a slow phase being present, but because of its weak intensity no attempt was made to analyze these runs according to a two-step model.

Kinetic experiments with TNS–pepsinogen are characterized by a rapid initial increase in fluorescent intensity whose amplitude corresponds to 25–30% of the total, followed at pH values below about 3.1 by a second phase of weaker amplitude in the sense of a decrease in intensity. An example of such a two-phase transient is shown in Figure 4. The rate constants obtained upon analysis of these experiments are presented in Figure 5. To facilitate comparison with the results obtained from intrinsic fluorescence, the same range of coordinates has been used in both Figures 3 and 5. The rate constants for both the rapid and slow phases exhibit a pronounced pH dependence, increasing as the pH decreases. But the extent of the increase and the actual values obtained are less than those found from intrinsic fluorescence of the native zymogen. The values of the rate constants for both phases in Figure 5 appear to pass through a maximum in the vicinity of pH 2 and may begin to decrease below this point. A slow phase was seen in only some runs at pH 3.10 and none was observed at pH 2.99. The amplitude of the slow phase increases from zero as the pH decreases from 3, attaining absolute values comparable to, but never exceeding, those of the rapid phase at the pH points at which two phases were detectable. The amplitude ratios are considered further under Discussion.

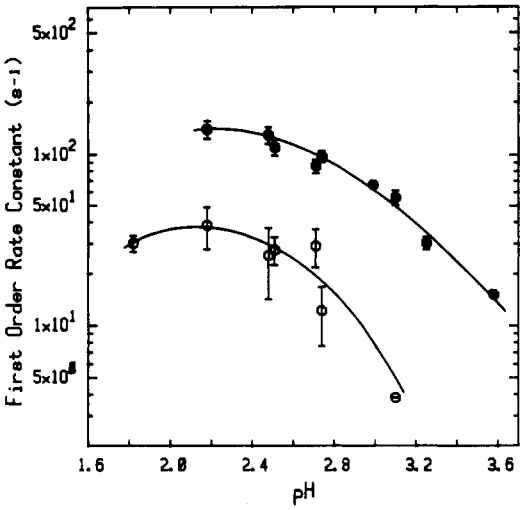

FIGURE 5: Rate constants for change in fluorescence of TNS–pepsinogen vs. pH. First-order rate constants (±SD) for the fast event (●) and for the slow event (○), determined as in Figure 4, are shown as a function of pH.

For both the native zymogen and the TNS derivative, no additional events were detected after the conclusion of those reported here until 2–5 s, depending on pH, had elapsed after mixing. This latter event we identify as the inception of conventionally detected activation. It was not pursued further in this study.

The dependence of our results on protein concentration was examined. The rate constants and fractional amplitudes are independent of concentration over a 2–3-fold range, which justifies our procedure of analyzing the transients according to first-order rate laws. Control experiments were done in which the excitation monochromator was set at a wavelength which was known to be above the cutoff of the emission filter, so that Rayleigh scattering could be observed. No changes in scattering intensity were found in the time ranges over which the fluorescence experiments yielded detectable transients. This was done for both the native zymogen and for the TNS derivative. Thus, even if the emission filters were to transmit some light at the incident wavelength, or if stray light reaching the observation cell were to be scattered into the detector, no contribution to the observed transients would appear. (Both emission filters were tested in an absorption spectrophotometer and found to have essentially 0% transmittance at the exciting wavelengths in question.)

Discussion

TNS-Cl reacts with amino and other nucleophilic groups of a protein. Pepsinogen has 11 amino groups, of which those on 9 lysyl residues and the one at the amino terminus are removed with complete activation of pepsinogen to pepsin. Thus, of the original amino groups, only that on Lys_{364}, seven residues from the carboxyl terminus, remains in pepsin (Se-

pulveda et al., 1975). The findings that TNS–pepsinogen contains one TNS group and that TNS–pepsin has virtually no free lysyl residues indicate that Lys_{364} carries the sole TNS label of the protein. The derivative activates at a rate and with a pH dependence that approximate the characteristics of the native zymogen (Figure 1), and the enzymatic activity obtained from the derivative is the same as that from the native zymogen.

The origins of the kinetic transients observed by intrinsic fluorescence of native pepsinogen are rather complex. The excitation wavelength chosen, 280 nm, excites both tyrosines and tryptophans. Much or all of the tyrosine excitation is most likely transferred by resonance energy transfer to tryptophan residues; in any case the emission filter with a cutoff at about 305 nm eliminates a significant portion of any tyrosine emission. Thus, we are observing predominantly tryptophan fluorescence. Changes in intensity of this parameter could be due either to an alteration of the local environments of the fluorophores themselves, induced by the exposure to acid (i.e., changes in local conformation), or to changes in juxtaposition of donor and acceptor residues involved in resonance energy transfer. The latter effects have the potential of being felt over distances of several nanometers and would therefore reflect more extensive conformational rearrangements. Our experiments have detected evidence for the occurrence of two pH-induced conformational changes in pepsinogen at pH values below about 2.6 and for one process above this pH. The faster process at low pH is very rapid indeed, approaching the limit of detectability of the stopped-flow apparatus.

The use of TNS as a fluorescent probe is conventionally based on the sensitivity of its fluorescent intensity (and the wavelength of its emission maximum) to the degree of hydrophobicity of its environment. The localization of the TNS moiety uniquely at Lys_{364} permits us to interpret results obtained with it with some confidence. If the gross structure of the pepsin moiety of porcine pepsinogen is not significantly altered upon activation, the environment of this residue can be understood upon examining the crystal structures of various homologous pepsins; the best defined of these is that of penicillopepsin (James & Sielecki, 1983). In this structure the corresponding position is located near the central waist of the enzyme opposite (i.e., on the back surface from) the active site cleft. The main chain of this residue is in one strand of a six-strand β-sheet which spans the amino-terminal and carboxyl-terminal domains. The fluorophore is thus in a position which may be responsive to conformational changes occurring in each domain.

As with the intrinsic fluorescence experiments, kinetic transients observed with TNS–pepsinogen also exhibit two phases over much of the pH range studied. In this case a rapid increase in intensity of relatively large extent is followed by a slower decrease with a weaker amplitude. None of the rate constants obtained with native pepsinogen is the same as that of TNS–pepsinogen at a given pH, except for a fortuitous crossing of the curves for the fast process at about pH 3.0 (compare Figures 3 and 5). The similarities between native pepsinogen and the labeled derivative may be summarized by noting that (a) both are activatable in a pH-dependent manner, (b) both exhibit two-phase transients at lower pH values and a single resolvable phase at higher pH values, and (c) the rates of these events are strongly pH dependent. Distinctions between the two proteins are in quantitative manifestations of these properties. These observations suggest that TNS–pepsinogen is a valid model to study the properties of the native zymogen. This notion implies that the two processes observed

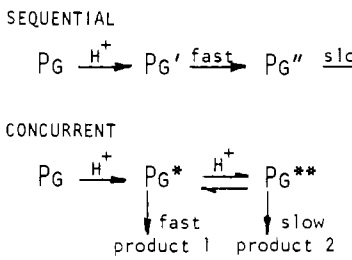

FIGURE 6: Models for early events of pepsinogen activation. In either model, the events are initiated by a protonation of pepsinogen (Pg) which is too fast to be observed. In the sequential model, this is followed by the fast event and then the slow event to produce, in sequence, Pg″ and Pg‴. In the concurrent model initial protonation brings the zymogen to a state (Pg*) that can undergo the fast transition; further protonation would bring it to a form (Pg**) that can undergo the slow transition. (In either model, the slow event is far faster than any irreversible step that leads to bond cleavage.)

in each protein reflect the same transformation, even though their rates differ between the two molecules. An alternative possibility is that intrinsic fluorescence in the native protein and that of the probe in the fluorescent derivative mirror entirely independent events, so that as many as four distinct conformational rearrangements are being detected upon exposure of pepsinogen (native or TNS derivative) to acid medium. With the information summarized above, the former explanation appears to be the more plausible.

The occurrence in many of the transients of two phases may be interpreted according to two alternative models, as illustrated in Figure 6. In further discussion, we shall focus attention on the TNS derivative, since kinetic parameters are better determined for this substance and we may be certain that we are dealing with uniquely identified processes. When the rate expression for the sequential model is worked out by using observable parameters such as optical absorption or fluorescence, the amplitude of the slow process, A_s, is given by eq 1 (Espenson, 1981). Here, F'' and F''' are the quantum

$$A_s = (F''' - F'')[\mathrm{Pg}]_0 k_f/(k_s - k_f) \qquad (1)$$

yields of Pg″ and Pg‴, respectively, $[\mathrm{Pg}]_0$ is the starting concentration of TNS–pepsinogen, and k_f and k_s are the rate constants for the fast and slow steps, respectively. Because the various runs were done with different experimental gains, A_s on the left side of eq 1 has been normalized to $A_s/(A_f + |A_s|)$, where the absolute value of A_s is taken in order to account for its negative sign. If the sequential model is valid, a plot of the normalized amplitude vs. $k_f/(k_s - k_f)$ should be linear and pass through the origin. This assumes that F'' and F''' are not profoundly pH dependent in the range of pH values examined, pH 2.18–2.74. A graph of our data cast in the formalism of eq 1 is shown in Figure 7. It is evident that these data are poorly correlated and cannot be analyzed to evaluate an intercept. Since the above criterion was not met, the sequential model was eliminated from further consideration.

The alternative model under discussion is one in which two separate starting materials undergo concurrent single-step first-order transformations to separate products (Moore & Pearson, 1981). In the present version of this model, two states of TNS-pepsinogen are in rapid protonic equilibrium with each other (Figure 6). If Pg* and Pg** are indeed related by protonic dissociation, then the amplitudes of the respective transients should be directly related to their relative proportions in solution at any given pH. They should therefore conform to a Henderson–Hasselbalch plot. We show such a plot in Figure 8, presented as the log of the ratio of the amplitude of the fast process to that of the slow process, using data from the same experiments as shown in Figure 7. The plot is linear

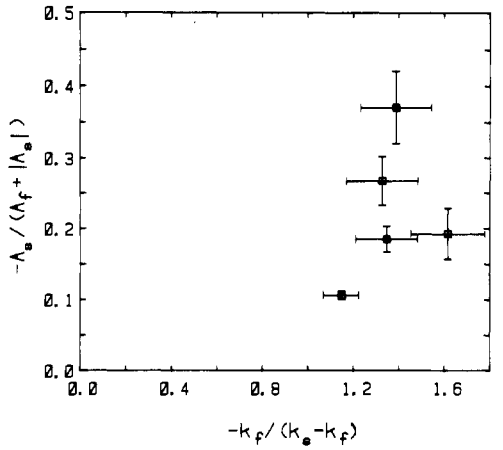

FIGURE 7: Test of kinetic data from TNS–pepsinogen for fit to the sequential model. The symbols have the meanings described in the text for eq 1. At each of five pH values the average, as well as the standard deviations in the x and y directions, evaluated from the results of two to four runs, is shown. The correlation coefficient for a linear regression of these data is 0.297.

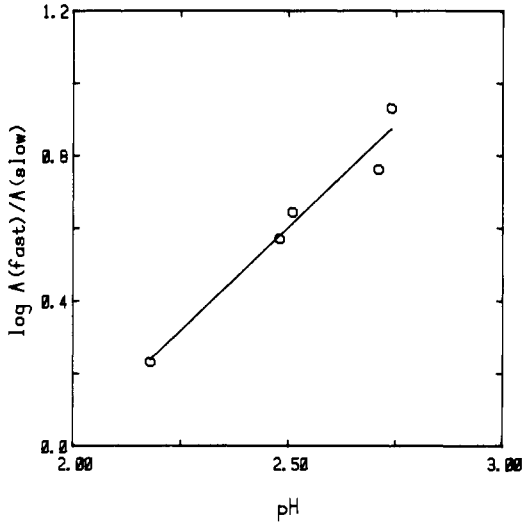

FIGURE 8: Test of kinetic data from TNS–pepsinogen for fit to the Henderson–Hasselbalch equation. The slope of the least-squares plot is 1.13 ± 0.14, and the correlation coefficient is 0.979.

with a correlation coefficient near 1 and has a slope of 1.13 ± 0.14. (Any differences in the quantum yields of Pg* and Pg** would appear in the plot of Figure 7 as a separate additive factor of the log of the ratio of the quantum yields. The position of the line would then be shifted up or down, but its linearity or its slope would not be affected.) No feature of the sequential model requires that the data fit a Henderson–Hasselbalch plot, but the concurrent model in Figure 6 does. Conversely, the concurrent model imposes no necessary relationship between the amplitudes and the rate constants, such as that of eq 1 obtained from the sequential model. For these reasons the Henderson–Hasselbalch plot is an adequate test of the concurrent model. Since the plot is linear, we conclude that the results are consistent with this model. The slope of the line in Figure 8 indicates that a single proton is involved in the interconversion of Pg* and Pg**. If the quantum yields for the two states do not differ greatly from one another, the pK_a for this dissociation process is approximately 2.0.

The concurrent model affords a unifying rationale for the circumstantial evidence that every kinetic parameter of activation has been found to be pH dependent. The catalytic step must have its pH dependence dictated by the pK_a values of the carboxyl groups at the active center, but this does not explain the pH dependence of all the other kinetic events of activation. For a long time the rate-limiting step of activation has been known to be similarly pH dependent (Herriott, 1938). One of us has observed that the dissociation of the activation peptide from nascent pseudopepsin, which must be the last event of activation, has a similar pH dependence (Twining et al., 1981). Even the energy of activation of the process varies with pH. [It declines from 18 kcal/mol at pH 2.0 to 11 kcal/mol at pH 3.25 (unpublished experiments).]

The simplest explanation for all of these findings is that there are two activation pathways, one predominating at pH 2 and the other at pH 3. Each event in one pathway has its counterpart in the other. Whenever we focus on any single event of activation, we see a combination of these two counterparts, the pH determining the proportionation between the two. We have no direct evidence that the fast and slow events we report here are integral to one or the other of those two pathways, respectively, but the fact that their pH dependence fits the pattern of every other observed step of activation supports their being in productive pathways.

In connection with this we note the recent report by Kageyama & Takahashi (1983) that pepsinogen can undergo initial unimolecular cleavage at either Leu_{16}–Ile_{17} or at Leu_{44}–Ile_{45}. Possibly these two cleavages terminate the two proposed activation pathways. While correlating nicely with our findings, this report of Kageyama and Takahashi must, nevertheless, be reconciled with the three-dimensional model of the protein that has been inferred from X-ray crystallographic models of microbial pepsins (Blundell et al., 1980; James & Sielecki, 1983). These models place Ile_{45}, the amino moiety of the proposed scissile bond of the zymogen, at the back of the molecule, well away from the active site.

Registry No. Pepsinogen, 9001-10-9.

References

Al-Janabi, J., Hartsuck, J. A., & Tang, J. (1972) *J. Biol. Chem. 247*, 4628–4632.

Auer, H. E., & Glick, D. M. (1983) *Fed. Proc., Fed. Am. Soc. Exp. Biol. 42*, 1951.

Blundell, T. L., Jones, H. B., Khan, G., Taylor, G., Sewell, B. T., Pearl, L. H., & Wood, S. P. (1980) *FEBS–Symp. No. 60*, 281–288.

Chow, R. B., & Kassell, B. (1968) *J. Biol. Chem. 243*, 1718–1724.

Epsenson, J. H. (1981) *Chemical Kinetics and Reaction Mechanisms*, pp 65–67, McGraw-Hill, New York.

Herriott, R. M. (1938) *J. Gen. Physiol. 22*, 65–78.

James, M. N. G., & Sielecki, A. R. (1983) *J. Mol. Biol. 163*, 299–361.

Kageyama, T., & Takahashi, T. (1983) *J. Biochem. (Tokyo) 93*, 743–754.

McClure, W. O., & Edelman, G. M. (1966) *Biochemistry 5*, 1908–1919.

McPhie, P. (1972) *J. Biol. Chem. 247*, 4277–4281.

Moore, J. W., & Pearson, R. G. (1981) *Kinetics and Mechanisms*, 3rd ed., pp 286–287, Wiley, New York.

Perlmann, G. E. (1964) *J. Biol. Chem. 239*, 3762–3766.

Savitsky, A., & Golay, M. J. E. (1964) *Anal. Chem. 36*, 1627–1639.

Sepulveda, P., Marciniszyn, J., Jr., Liu, D., & Tang, J. (1975) *J. Biol. Chem. 250*, 5082–5088.

Twining, S. S., Sealy, R. C., & Glick, D. M. (1981) *Biochemistry 20*, 1267–1272.

Wang, J. L., & Edelman, G. M. (1971) *J. Biol. Chem. 246*, 1185–1191.